Brain Pathology 10: 260-272(2000)

RESEARCH ARTICLE

Microglial Activation and Neuronal Apoptosis in Bornavirus Infected Neonatal Lewis Rats

Herbert Weissenböck[1,2], Mady Hornig[1], William F. Hickey[3], W. Ian Lipkin[1]

[1] Emerging Diseases Laboratory, University of California, Irvine, California
[2] Institute of Pathology, University of Veterinary Medicine, Vienna, Austria
[3] Department of Pathology, Dartmouth Medical School, Hanover, New Hampshire

Lewis rats neonatally infected with Borna disease virus have a behavioral syndrome characterized by hyperactivity, movement disorders, and abnormal social interactions. Virus is widely distributed in brain; however, neuropathology is focused in dentate gyrus, cerebellum, and neocortex where granule cells, Purkinje cells and pyramidal cells are lost through apoptosis. Although a transient immune response is present, its distribution does not correlate with sites of damage. Neuropathology is instead colocalized with microglial proliferation and expression of MHC class I and class II, ICAM, CD4 and CD8 molecules. Targeted pathogenesis in this system appears to be linked to microglial activation and susceptibility of specific neuronal populations to apoptosis rather than viral tropism or virus-specific immune responses.

Introduction

Borna disease (BD) in its classic form is a nonsuppurative meningoencephalitis of ungulates confined to central Europe. The illness is due to infection with Borna disease virus (BDV) (35, 51), the prototype of a new family, *Bornaviridae*, within the nonsegmented negative-strand RNA viruses (7, 55). Recent studies indicate that the agent may also produce subtle or inapparent infection in a wide variety of warmblooded animal species in greater Europe, Asia, and North America (2, 4, 5, 20, 21, 29, 38, 48).

Corresponding author:
Dr. W. Ian Lipkin, Emerging Diseases Laboratory, 3101 Gillespie Neuroscience Research Facility, University of California, Irvine, CA 92697-4292. ; Tel.: (949)824-6193; Fax: (949)824-1229; E-mail: ilipkin@uci.edu

Animal models of Borna disease are established in birds, rodents, lagomorphs, ungulates, and primates (51). The best characterized of these model systems is the adult Lewis rat where infection results in meningoencephalitis and characteristic behavioral abnormalities linked to dopamine neurotransmitter disturbances (22, 23, 35, 39, 59, 62). Less attention has been focused on neonatal Lewis rats where infection results in hippocampal and cerebellar degeneration without robust infiltrative immunopathology (3, 9, 17, 39, 52, 53). The neonatal model is intriguing because some features of the syndrome observed in Lewis rats, including hyperactivity, stereotypies, abnormal righting reflexes (25), and disturbed play behavior (44), are reminiscent of human neuropsychiatric disorders, including autism. Recently, histologic and molecular analysis of neonatally infected rats revealed a transient infiltration of chronic inflammatory cells and production of proinflammatory cytokine mRNA expression (25, 54). Here we report detailed investigation of the neuropathology of this model. Our findings indicate that apoptosis contributes substantively to degeneration of the cerebellum, hippocampal formation, and neocortex, and points to selective vulnerability of specific cell populations and circuits during central nervous system (CNS) development.

Materials and Methods

Infection of Animals. Lewis rat pups (progeny of pregnant dams, Charles River Laboratories) were inoculated within 12 hours of birth by intracerebral (i.c.) injection into the right hemisphere of 5×10^3 tissue culture infectious units of the fourth brain passage in neonatal Lewis rats of BDV strain He/80-1 (NBD rats) or phosphate-buffered saline (PBS, NL rats) in a total volume of 50 μl. At 2, 3, 4, 5, 6, 12, 24, and 52 weeks post inoculation (p.i.) 3 to 5 animals per group were anesthetized with methoxyfluorane (Pitman-Moore) and perfused with PBS followed by 4% buffered paraformaldehyde in 0.1 M phosphate buffer, pH 7.4.

Antibody	Specificity	Host	Dilution	Reference/Vendor
anti-p40	nucleoprotein of Borna Disease Virus (BDV)	rabbit	1:3000	Reference 6
anti-GFAP	glial fibrillary acidic protein	rabbit	1:800	Dako
anti-iNOS	nitric oxide synthase type II (inducible)	rabbit	1:500	Transduction Laboratories
anti-IL1 beta	interleukin 1 beta	goat	1:200	Santa Cruz Biotechnology
5F10	vascular cell adhesion molecule-1 (VCAM-1)	mAb	1:100	Berkeley Antibody Company
OX 19	CD5 on T cells	mAb	undiluted	Reference 12
R.73	alpha/beta T cell receptor	mAb	undiluted	Reference 26
W3/25	CD4	mAb	undiluted	Reference 64
OX 8	CD8 alpha	mAb	undiluted	Reference 28
341	CD8 beta	mAb	1:200	Pharmingen
3.2.3	NK cells	mAb	undiluted	Reference 10
OX 42	CD11 b/c on microglia and macrophages	mAb	undiluted	Reference 49
I1.69	MHC-I	mAb	undiluted	Reference 30
OX 6	MHC-II	mAb	undiluted	Reference 36
TLD-4C9	intercellular adhesion molecule-1 (ICAM-1)	mAb	undiluted	Reference 14
TLD-3A12	platelet endothelial cell adhesion molecule (PECAM)	mAb	undiluted	Reference 65
TLD-1F5	perivascular cell	mAb	undiluted	Reference 14
biotinylated anti-rat IgG	rat IgG, B-cells, plasma cells	goat	1:100	Vector Laboratories

Table 1. Antibodies used for immunocytochemistry.

Histology and Immunohistochemistry. Perfused brains were removed and 2 mm coronal slices postfixed by immersion in paraformaldehyde perfusate at 4°C for 30 min. After rinsing in 0.2 M phosphate buffer, tissue was cryoprotected in 30% sucrose, embedded in mounting media (OCT, Sakura Finetek, Torrance, CA), and frozen at -70°C. Twenty micrometer coronal sections were collected onto Vectabond-coated slides (Vector Laboratories, Burlingame, CA) in series through frontal and olfactory cortex; striatum; nucleus accumbens; parietal; temporal and occipital cortex; thalamus and hypothalamus; hippocampus; midbrain; medulla oblongata; and cerebellum. For paraffin embedding, brains were fixed in 4% paraformaldehyde until processing. Five μm coronal sections of the described areas were mounted on coated slides.

Tissue sections were stained with hematoxylin and eosin (H&E) for histological assessment. The primary antibodies used for immunohistochemistry (IHC), their specificities, and dilutions are listed in Table 1. Secondary antibodies were biotinylated anti-rabbit IgG, biotinylated anti-goat IgG (dilution 1:200) and biotinylated anti-mouse IgG (rat adsorbed, dilution 1:100) (all Vector Laboratories). Primary and secondary antibodies were incubated overnight at 4°C. Washes were done in 0.5 M Tris buffer (pH 7.6) containing 1% fetal calf serum (FCS). The avidin-biotin-complex technique (ABC) using the Vectastain Elite kit (Vector Laboratories) was applied according to manufacturer's instructions. Diaminobenzidine (DAB) was used as chromogen. Sections were counterstained with hematoxylin or left unstained. The intensity and spread of specific staining was assessed using the following score systems: *Immune cell markers* (R.73, W 3/25, OX8, 3.2.3): -, no positive cells; (+), single positive cells; +, up to 25 positive cells; ++, 26 to 50 positive cells; +++, more than 50 positive cells per 200× field. *OX42*: -, no activated microglia cells; +, up to 15 activated microglia cells; ++, 16 to 30 activated microglia cells; +++, over 30 activated microglia cells per 500× field. *GFAP*: -, no reactive astrocytes; +, up to 5 reactive astrocytes; ++, 6 to 10 reactive astrocytes; +++, over 10 reactive astrocytes per 200× field. *All others*: +++, intense, widespread staining; ++, heterogeneous staining; +, light, limited staining.

Terminal deoxynucleotidyl transferase (TdT) dUTP-Biotin Nick End Labeling (TUNEL). Cells with fragmented DNA were labeled by TUNEL (15). Briefly, tissue was treated with 10 μg/ml proteinase K (Boehringer Mannheim) for 5 min at 37°C, washed in PBS, fixed in paraformaldehyde, treated with 0.3% hydrogen peroxide in methanol, dehydrated through a graded series of alcohols and air dried. Sections were covered with a mixture of 1 mM biotinylated 16-dUTP (Boehringer Mannheim, Indianapolis, IN), 10 mM dATP (Pharmacia, Piscataway, NJ), TdT (Promega, Madison, WI), 5× TdT buffer (Promega), and dH_2O and

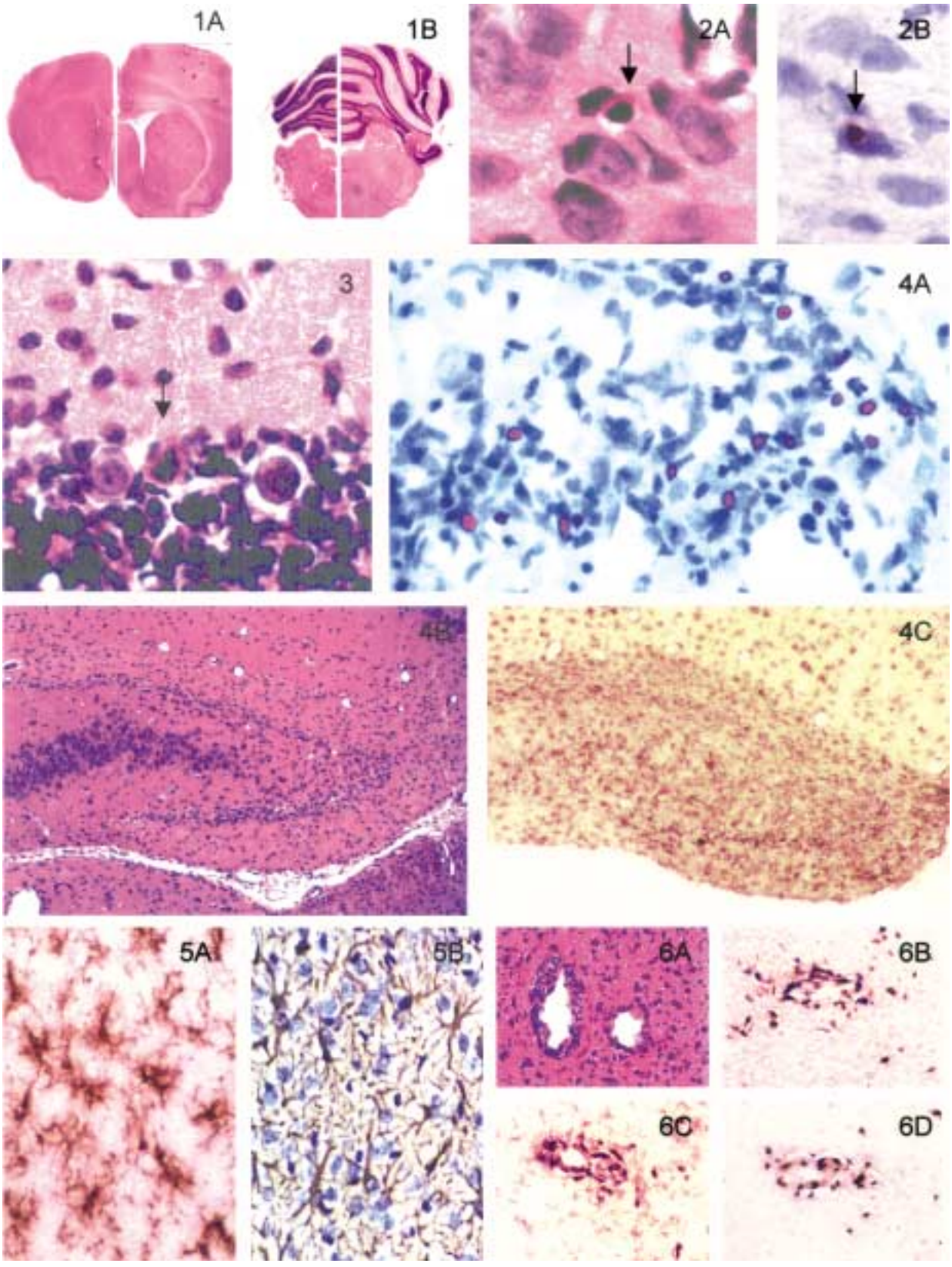
1A
1B
2A
2B
3
4A
4B
4C
5A
5B
6A
6B
6C
6D

incubated for 1 h at 37°C. After rinsing, the reaction was visualized using the Vectastain Elite ABC kit (Vector Laboratories) as described above. Cells were determined to be positive on the basis of intense brown nuclear staining. Intensity of apoptotic cell death was assessed by the following score system: +, up to 10 positive nuclei/200× field, ++, 11 to 30 positive nuclei/200× field, +++, more than 30 positive cells/200× field.

In Situ Hybridization (ISH). BDV genomic and subgenomic transcripts were localized by ISH. Probes were generated from plasmid pcD5 containing the complete sequence of BDV phosphoprotein (P) cloned into pcDNA 3 (Invitrogen, Carlsbad, CA). Digoxigenin (DIG)-labeled single stranded RNA probes were obtained by *in vitro* transcription of the HindIII linearized plasmid using SP6 polymerase (probe for mRNA) and the EcoR1 linearized plasmid with T7 polymerase (probe for genomic RNA).

Pilot experiments demonstrated that paraffin embedded tissue provided superior anatomic resolution; thus, only studies with paraffin sections are described. Sections were deparaffinized in xylene, rehydrated through graded alcohols, fixed in paraformaldehyde for 5 min, treated with 20 μg/ml proteinase K (Boehringer Mannheim) at 37°C for 30 min and 0.3% Triton X (Boehringer Mannheim) for 5 min, fixed again in paraformaldehyde for 5 min, dehydrated through graded alcohols and air dried. Methods for hybridization were as previously reported (34). The sections were washed with TNE (10 mM Tris, pH 7.5; 0.5M NaCl, and 1 mM EDTA) at 37°C for 1 h, treated with 10 μg/ml RNAse A (Calbiochem, La Jolla, CA) in TNE and with 0.5 SSC at 37°C for 15 min. Slides were incubated with a blocking solution (1% FCS, 1% bovine serum albumin and 0.3% Tween 20 in PBS) for 1 h, followed by alkaline phosphatase-conjugated anti-DIG Fab fragments (Boehringer Mannheim), diluted 1:300 in blocking solution for 3 h. After rinsing in PBS specific hybrids were detected by overnight incubation with nitro blue tetrazolium chloride and 5-bromo-4-chloro-3-indolyl phosphate (NBT/BCIP, Boehringer Mannheim). Hybridization with anti-genomic T7 probe resulted in signal confined to nuclei; hybridization with anti-mRNA SP6 probe yielded predominantly cytoplasmic signal.

Combined ISH and IHC to Determine Cellular Distribution of BDV. Paraffin sections were processed for ISH as described above with the addition of a 10 min incubation in 0.3% hydrogen peroxide in methanol prior to treatment with proteinase K. Following hybridization, antibodies to GFAP (Dako, Carpinteria, CA; 1:800) and ED-1 (Serotec, Oxford, UK; 1:2000) were incubated simultaneously with anti-DIG Fab fragments. Slides were incubated with biotinylated anti rabbit IgG (Vector Laboratories; 1:200) or biotinylated anti mouse IgG (Vector Laboratories; 1:200) for 1 h at 37°C, rinsed in Tris-buffered saline (TBS; 50 mM Tris, ph 7.5, 100 mM sodium chloride) incubated with ABC reagent for 1 h at 37°C, rinsed again and covered with DAB for 5 min. After rinsing in TBS, slides were covered with NBT/BCIP, incubated overnight, rinsed again, and coverslipped with Gelmount (Biomeda, Foster City, CA).

Results

Neuropathology. Brains of NBD rats were smaller than those of NL rats after 4 weeks p.i. The reduction of

Figure 1. Thinning of cerebral cortex and cerebellar molecular layer in an NBD rat. Coronal sections: striatum of an NBD rat (**A**, left) and NL rat (**A**, right), 6 weeks p.i.; cerebellum and brainstem of an NBD rat (**B**, left) and NL rat (**B**, right), 12 weeks p.i. Note preservation of striatum (A) and cerebellar foliation, and brainstem (**B**). H&E; magnification, ×3

Figure 2. Neuronal apoptosis in an NBD rat at 4 wks p.i. Cortical neuron with nuclear condensation and shrinkage and cytoplasmic hypereosinophilia (arrow). H&E (**A**). TUNEL-positive cortical neuron (arrow) (**B**). Magnification, ×1000

Figure 3. Apoptosis of a Purkinje cell (arrow) in an NBD rat. Note nuclear condensation, shrinkage and hypereosinophilia of cytoplasm. NBD rat, 4 weeks p.i.; H&E; magnification, ×500

Figure 4. Evolution of dentate gyrus pathology in NBD. (**A**) TUNEL-positive apoptotic DG granule cells at 4 weeks p.i.; magnification ×450. (**B**) loss of DG granule cells at 5 weeks p.i.; H&E; magnification, ×60. (**C**) marked microgliosis in dentate gyrus at 6 weeks p.i.; OX42 IHC; magnification, ×60

Figure 5. Proliferation and activation of microglia (**A**, mesencephalon) and astrocytes (**B**, cortex) in an NBD rat at 6 weeks p.i. (**A**) OX42 IHC; magnification, ×220. (**B**) GFAP IHC; hematoxylin counterstain; magnification, ×240

Figure 6. Immune cell infiltrates in an NBD rat at 4 weeks p.i. (**A**) Perivascular cuffing and diffuse microgliosis in frontal cortex; H&E; magnification, ×100. (**B**) Pan T-cell marker (R 73). (**C**) CD4 marker (W3/25). (**D**) CD8 marker (OX8). Magnification, ×140

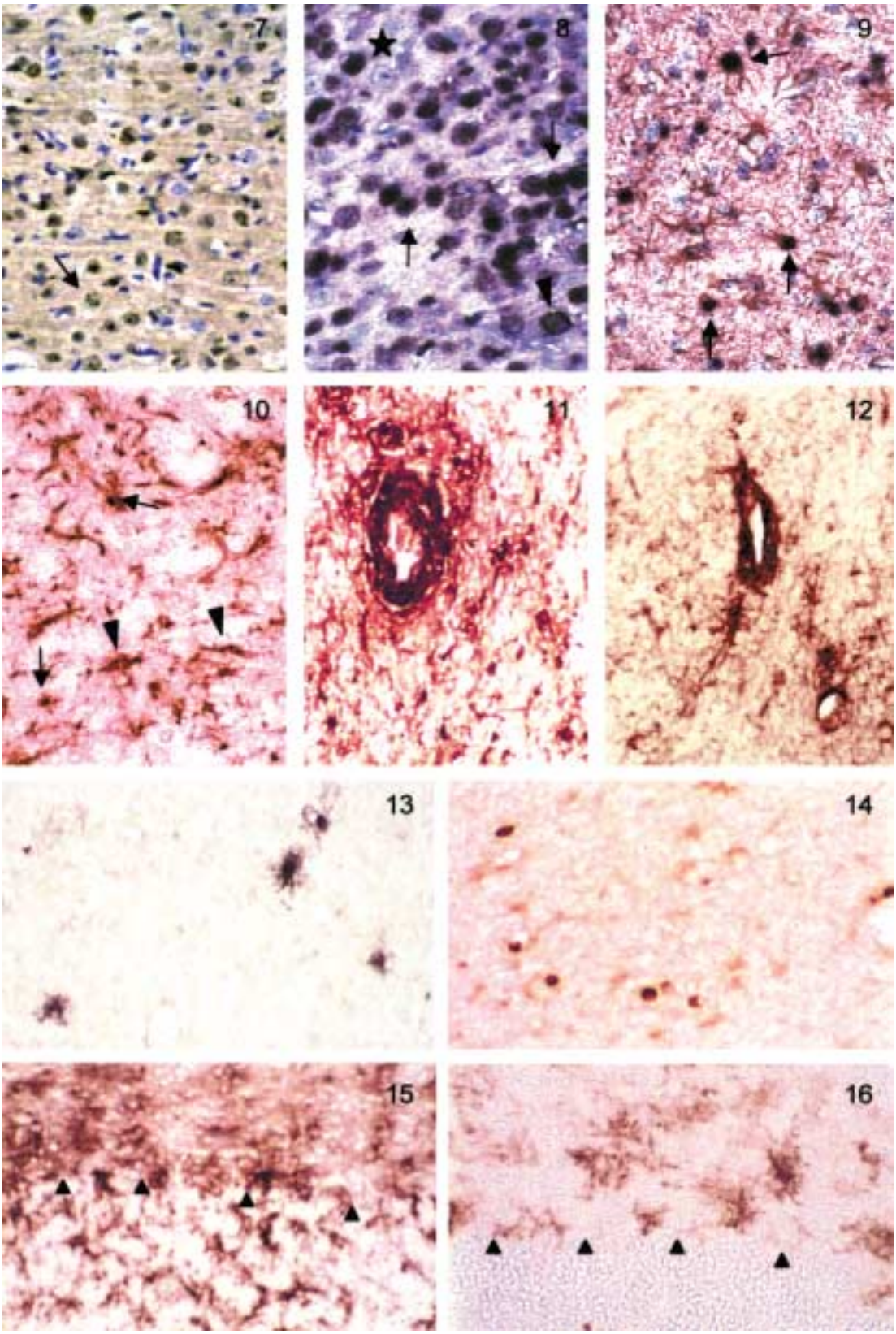
7
8
9
10
11
12
13
14
15
16

size was primarily due to thinning of cortex and involution of hippocampus and cerebellum (Figure 1).

No overt neuropathological changes were observed at 2 weeks p.i.; however, at 3 weeks p.i., apoptotic neurons were found in cerebral cortex, dentate gyrus (DG), and the Purkinje cell layer of cerebellum. Apoptotic cells were characterized by shrinkage, hypereosinophilic cytoplasm, nuclear pyknosis and karyorrhexis, and signal on TUNEL assay (Figure 2, 3, and 4A). Apoptotic changes peaked at four weeks p.i., with most marked pathology in DG and cortical layers 5 and 6 of retrosplenial and cingulate cortex. The number of apoptotic cells gradually decreased through 5 to 6 weeks p.i. At 6 wks p.i. granule cells in DG were largely replaced by activated microglial cells and reactive astrocytes (Figure 4B and 4C). Marked microgliosis and moderate astrogliosis occurred in all brain regions after 4 wks p.i. and was present at the last timepoint examined, 52 wks p.i. (Figure 5A and 5B). In cerebellum of NBD rats, several observations were made: only scattered Purkinje cells were observed after 6 weeks p.i.; the molecular layer was markedly thinner with more modest thinning of the internal granular layer (Figure 1B); and white matter appeared normal. At 4 weeks p.i., mononuclear inflammation was observed in leptomeninges, perivascular spaces and neuropil of NBD rats, focused predominantly in the cingulate, frontal and parietal cortices (Figure 6A). Immunohistochemical characterization of infiltrates revealed that the majority were T cells (as reflected by staining with antibodies to CD 5 or the alpha/beta T cell receptor) (Figure 6B) with smaller numbers of NK cells, monocytes/macrophages, perivascular cells, and B cells (3.2.3, OX 42, TLD 1F5, and anti-rat IgG staining, respectively). Overall numbers of CD4+ and CD8+ cells were similar (Figure 6C and 6D); however, CD4+ cells were present primarily in the meninges and perivascular spaces, whereas CD8+ cells were diffusely distributed in the neuropil.

Neuroanatomical Distribution of BDV Nucleoprotein and BDV RNA. At 2 weeks p.i. viral nucleoprotein was readily detected in cerebral and olfactory cortex and hippocampus of NBD rats. However, layer IV and the cerebellar granule cell layer contained minimal nucleoprotein and only few positive cells were present in striatum, nucleus accumbens or thalamus. The majority of stained cells were neurons, where protein appeared within Joest-Degen intranuclear inclusion bodies, entire nuclei, or nuclei and cytoplasm, including neuronal processes. Rare astrocytes, ependymal cells, and oligodendrocytes were also positive at 2 wks p.i. At 4 to 6 weeks p.i., staining was more diffuse, with distribution

Figure 7. Viral nucleoprotein in frontal cortex of an NBD rat at 4 weeks p.i. Note staining of neuronal nuclei and neuropil. Arrow indicates numerous intranuclear inclusion bodies. p40 IHC; hematoxylin counterstain; magnification, ×200

Figure 8. Viral phosphoprotein mRNA in frontal cortex of an NBD rat at 4 weeks p.i. Arrows, nuclei; arrowhead, cytoplasm; asterisk, Joest-Degen inclusion bodies; ISH; hematoxylin counterstain; magnification, ×200

Figure 9. Viral genomic RNA in astrocytes in frontal cortex of an NBD rat at 6 weeks p.i. Arrow indicates double-labeling with GFAP IHC +ISH; hematoxylin counterstain; magnification, ×200

Figure 10. MHC-I expression on endothelial cells (arrowheads) and microglial cells (arrows) in frontal cortex of an NBD rat at 4 weeks p.i.; I1.69 IHC; magnification, ×210

Figure 11. MHC-II expression on perivascular inflammatory cells and microglial cells in frontal cortex of an NBD rat at 4 weeks p.i.; OX6 IHC; magnification ×210

Figure 12. ICAM-1 expression on blood vessels and microglia in frontal cortex of an NBD rat at 4 weeks p.i.; TLD-4C9 IHC; magnification ×210

Figure 13. IL-1 beta expression in single microglial cells in frontal cortex of an NBD rat at 4 weeks p.i.; IHC; magnification ×250

Figure 14. iNOS expression in single parenchymal macrophages in frontal cortex of an NBD rat at 4 weeks p.i.; IHC; magnification ×250

Figure 15. CD4 expression on microglial cells in granule cell layer and molecular layer of cerebellum (arrowheads indicate Purkinje cell layer) of an NBD rat at 4 weeks p.i.; W3/25 IHC; magnification ×250

Figure 16. CD8 expression on microglial cells in the molecular layer of cerebellum of an NBD rat at 4 weeks p.i.; OX8 IHC; magnification ×250

of nucleoprotein in both neuronal and glial processes (Figure 7). The overall staining intensity gradually decreased from 28 to 52 weeks p.i. Viral genomic RNA was localized as multiple sharp dots or as staining of the entire nucleus in cell populations containing viral nucleoprotein. Viral mRNA was abundant in cytoplasm (Figure 8). Brains of NL rats did not stain for viral nucleoprotein or hybridize with probes for detection of BDV transcripts (data not shown).

Phenotypic Characterization of Cells in Brain Harboring Viral Sequences. Neurons, ependymal cells, and oligodendroglia containing BDV genomic RNA and mRNA were readily identified by morphology and location. No viral sequences were detected in epithelial cells of choroid plexus, infiltrating inflammatory cells or endothelial cells. Viral replication in astrocytes and microglia could not be unequivocally addressed using morphological and anatomic criteria. Thus, double-labeling approaches were pursued with DIG-labeled probes for detection of genomic RNA through ISH, and antibodies to GFAP or ED-1 as markers of astrocytes or microglia, respectively. Infected astrocytes were detected (Figure 9); BDV RNA was not found in microglia.

Timecourse of Expression of MHC, PECAM-1, ICAM-1, IL1-beta and iNOS in Brains of NBD and NL rats. MHC Class I molecules were present at similar levels on endothelial cells of NBD and NL rats at 2 wks p.i. After 4 wks p.i., MHC Class I was detected at higher levels in endothelial cells of NBD rats. Additionally, after 4 weeks p.i., NBD rats expressed MHC Class I on microglial cells and rare astrocytes and neurons. MHC Class I expression peaked between weeks 4 and 6 (Figure 10) and decreased thereafter through the latest timepoint examined (52 wks p.i.). MHC Class II was present at similar levels in meninges and choroid plexus of NBD and NL rats at 2 wks p.i. In NL rats levels and distribution of MHC Class II were similar through 52 wks p.i. In contrast, levels of MHC Class II in NBD rats were higher after 4 wks p.i. and expression extended to microglia and inflammatory cells (Figure 11). Microglial MHC Class II expression decreased rapidly thereafter and was difficult to detect after 6 weeks p.i.

PECAM-1 was expressed constitutively on endothelial cells of NBD and NL rats at all timepoints. ICAM-1 was present on endothelial cells of large blood vessels in NBD and NL rats at 2 wks p.i. After 4 wks p.i., levels of ICAM-1 were increased on endothelial and other vascular and perivascular cells of NBD rats (Figure 12) with most prominent staining in cerebral cortex, hippocampus, and cerebellum. Thereafter, ICAM-1 expression decreased, reaching control values by 24 wks p.i. In NBD rats, IL-1beta immunoreactivity was detected at 4 weeks p.i. in perivascular inflammatory cells and disseminated clusters of microglial cells (Figure 13), predominantly in cortical regions. Rare macrophages in cortices of NBD rats stained for iNOS at 4 wks p.i. (Figure 14; regional and serial analysis of immune and cell surface markers, Table 2; summary of serial changes, Table 3).

CD4 and CD8 Molecules on Microglial Cells. CD4 was readily detected on perivascular cells, meningeal cells, rare cells in choroid plexus, and microglia of control and infected rats throughout the 52 wk observation period. From 4 wks through 52 wks p.i., NBD rats had markedly elevated CD4 expression on the majority of activated microglial cells (Figure 15). Initial efforts to stain CD8 cells employed the antibody OX8 which detects the alpha chain of the CD8 molecule. Neither endogenous nor infiltrating cells exhibiting OX8 staining were observed in control rats. In contrast, OX8+, activated microglia were present in NBD rats at 4 wks p.i. in cingulate and retrosplenial cortices, DG, and molecular layer of cerebellum (Figure 16). OX8+ microglia also stained with antibodies specific for CD8b, confirming the presence of the beta chain of the CD8 molecule on activated microglia. After 6 wks p.i., CD8 expression was limited to cells in the cerebellar molecular layer and was not detected at all after 24 wks p.i. (regional and serial analysis of immune and cell surface markers, Table 2; summary of serial changes, Table 3).

Discussion

Neonatal inoculation of Lewis rats with BDV results in persistent infection of neurons, astrocytes, oligodendroglia, and ependymal cells. The distribution of virus is more diffuse in brains of NBD rats than adult infected rats, where BDV is focused primarily in limbic circuits. Interestingly, two neuronal populations infected in adult rats, neurons of layer IV of cortex and granule cells of cerebellum (18), appear to be spared in NBD rats. The reason for this age-related discrepancy in neuronal susceptibility is unknown.

Although infected neurons are present throughout the brain of NBD rats, damage is confined to DG granule cells, Purkinje cells, and cortical pyramidal neurons. These cells undergo apoptotic cell death, as demonstrated by morphologic criteria (Figures 2 and 3), positive

Antigen	Location	2 wks p.i. NL	2 wks p.i. NBD	4 wks p.i. NL	4 wks p.i. NBD	5 wks p.i. NL	5 wks p.i. NBD	6 wks p.i. NL	6 wks p.i. NBD	24 wks p.i. NBD	52 wks p.i. NBD
CD 11b, CD 18 (OX 42)[1]	vessels	+	+	+	+	+	+	+	+	+	+
	parenchyma	+	+	+	+++	+	+++	+	+++	++	++
GFAP	vessels	-[2]	+	-	+++	-	+++	-	++	+	+
	parenchyma	-	+	-	+++	-	+++	-	++	+	+
TcR α/β	vessels	-	-	-	+++	-	+	-	+	(+)	(+)
(R 7.3 Ab)	parenchyma	-	-	-	+++	-	+	-	+	(+)	(+)
CD 5	vessels	-	-	-	+++	-	+	-	+	ND	ND
(OX 19 Ab)	parenchyma	-	-	-	+++	-	+	-	+	ND	ND
CD 4[3] on lymphocytes	vessels	-	-	-	+++	ND	+	-	+	-	-
(W3/25 Ab)	parenchyma	-	-	-	++	ND	+	-	(+)	(+)	(+)
CD 8 on lymphocytes	vessels	-.	-	-	++	ND	+	-	(+)	-	-
(OX8 Ab)	parenchyma	-	-	-	+++	ND	++	-	+	(+)	(+)
NK cells	vessels	-	-	-	+	ND	(+)	-	(+)	-	-
(3.2.3 Ab)	parenchyma	-	-	-	+	ND	+	-	+	(+)	(+)
TLD-1F5	vessels	-	-	+	+	+	+	+	+	ND	ND
(ED 2 Ab)	parenchyma	-	-	-	-	-	-	-	-	ND	ND
anti-IgG[4]	vessels	n.a.	n.a.	n.a.	n.a.	n.a.	n.a.	n.a.	n.a.	n.a.	n.a.
	parenchyma	(+)	+	+	+	(+)	+	(+)	+	+	+
MHC-I	vessels	+	+	+	+++	+	+++	+	+++	++	++
(I 1.69 Ab)	parenchyma	-	-	-	++	-	++	-	+	+	+
MHC-II	vessels	-	-	-	+++	-	+	-	+	-	-
(OX6 Ab)	parenchyma	-	-	-	+++	-	+	-	+	+	(+)
PECAM-1	vessels	+++	+++	+++	+++	+++	+++	+++	+++	ND	ND
(TLD-3A12 Ab)	parenchyma	-	-	-	-	-	-	-	-	ND	ND
ICAM-1	vessels	(+)	(+)	(+)	+++	ND	ND	(+)	++	+	+
(TLD-4C9 Ab)	parenchyma	-	-	-	+	ND	ND	-	-	-	-
IL-1 beta	vessels	-	-	-	+	-	-	-	-	-	-
	parenchyma	-	-	-	+[5]	-	(+)	-	-	-	-
iNOS	vessels	-	-	-	+	-	-	-	-	-	-
	parenchyma	-	-	-	+	-	(+)	-	-	-	-
CD 4 on microglia	vessels	n.a.	n.a.	n.a.	n.a.	n.a.	n.a.	n.a.	n.a.	n.a.	n.a.
(W3/25 Ab)	parenchyma	+	+	+	+++	+	+++	+	+++	+++	+++
CD8 on microglia	vessels	n.a.	n.a.	n.a.	n.a.	n.a.	n.a.	n.a.	n.a.	n.a.	n.a.
(OX8 Ab)	parenchyma	-	-	-	++	-	++	-	+	-	-

Abbreviations. NL = normal rats; NBD = neonatal Borna disease virus infected rats; ND: not done; n.a.: not applicable

Scoring Systems:

For immune cell markers (R.73, W 3/25, OX8, 3.2.3):
- : negative
(+) : single positive cells or traces of specific reaction
\+ : up to 25 positive cells
++ : 26 to 50 positive cells
+++ : more than 50 positive cells per 200× field.

For OX 42:
- : negative
(+) : single positive cells or traces of specific reaction
\+ : 15 activated microglia cells
++ : 16 to 30 activated microglia cells
+++ : over 30 activated microglia cells per 500× field

For GFAP:
- : negative
(+) : single positive cells or traces of specific reaction
\+ : up to 5 reactive astrocytes
++ : 6 to 10 reactive astrocytes
+++ : over 10 reactive astrocytes per 200× field

For all others:
\+ : light, limited staining
++ : heterogeneous staining
+++ : intense, widespread staining

[1] positive cells have morphology of microglial cells and macrophages; only single macrophages in neuroparenchyma
[2] normal astrocyte population, no reactive morphology
[3] CD4 constitutively expressed on perivascular cells
[4] diffuse neuropil staining slightly increased compared to controls; single plasma cells in meninges and neuropil
[5] expression on single cells with microglial and macrophage morphology

Table 2. Serial changes in immune and cell surface markers following neonatal BDV infection.

Pathologic Feature	2 wks	4 wks	6 wks	24 wks	52 wks
reduction of brain size	-	+	++	+++	+++
apoptosis of neurons	+	+++	+	-	-
immune cell infiltration	(+)	+++	+	(+)	(+)
microgliosis and astrocytosis	-	++	+++	+++	+++
viral protein and RNA	++	+++	+++	+++	++
degeneration of dentate gyrus	-	++	+++	+++	+++
MHC-I expression	+	+++	++	++	++
MHC-II expression	-	+++	+	(+)	(+)
CD4 expression on microglia	-	+++	++	++	++
CD8 expression on microglia	-	++	+	(+)	-

score: - : not present
(+) : single positive cells
+ : mild
++ : moderate
+++ : severe

Table 3. Summary of changes in Lewis rat brain following neonatal BDV infection.

TUNEL assays (Figures 2 and 4) and recent work indicating RNA expression profiles remarkable for increased caspase 1, increased Fas, and decreased bcl-x (25). Although DG and cerebellar pathology are previously reported (3, 9, 13, 52), our data provide insights into mechanisms responsible for damage in this model.

The selective vulnerability of these three distinct cell populations to apoptosis is intriguing. Two of the vulnerable cell types, DG granule cells and Purkinje cells, express calcium binding proteins, including calbindin, calretinin, and parvalbumin (16, 57). Calcium participates in apoptosis and excitotoxic signalling cascades (63, 66). Furthermore, regional differences in calcium-binding protein expression may contribute to neuroprotection in some models of apoptosis (45) but contribute to vulnerability to programmed cell death in other systems (31, 47). Thus, one basis for increased susceptibility to apoptosis of selected neuronal populations in NBD rats may be regional differences in calcium-binding protein activity. Another potential explanation for the selective vulnerability of DG is that microneurons, such as granule cells in cerebellum and DG, divide postnatally (1) and may be more susceptible to damage than postmitotic neurons. Although DG granule cells are infected in this model, cerebellar granule cells are spared (3). The reduction in cerebellar size primarily reflects the loss of Purkinje cells and their dendrites in the molecular layer. We appreciated only modest apoptosis of uninfected cerebellar granule cells (25); this may be explained by an indirect effect due to loss of their synaptic connections with Purkinje cells.

Neuroendocrine disturbances may also contribute to DG damage in NBD rats. In normal rats, adrenalectomy results in apoptosis of DG granule cells, presumably due to initiation of a protease cascade resulting in apoptosis when glucocorticoid or mineralocorticoid receptors in DG are not occupied by their endogenous ligands (58). Adrenals of 5 NBD rats with DG pathology appeared histologically normal and contained no viral protein by immunohistochemical analysis (data not shown). These findings suggest that overt adrenal damage is unlikely to contribute to the syndrome; however, functional assays of adrenal function were not performed. Nonetheless, it is established that Lewis rats have a blunted hypothalamic-pituitary-adrenal (HPA) axis, resulting in impaired glucocorticoid release in response to stressors and inflammatory challenges (60, 61). The inability of neonatally infected Lewis rats to adequately react to the stress of infection may result in glucocorticoid levels that are insufficient to maintain the integrity of the infected DG. This hypothesis is supported by preliminary data from our laboratory indicating that DG damage is more modest in neonatally infected Fischer rats, a strain with intact HPA axis (32). The observation that the extent of neuropathology may vary in identical species infected with identical agents but differing in neuroendocrine responses provides an interesting model for investigating host-pathogen interactions.

Proliferation and activation of glial cells, particularly astroglia, has been reported in neonatal BD (3, 9, 54). We also found astroglial proliferation but were more impressed by proliferation and activation of microglia. Proliferation of activated microglia and astrocytes is a common sequela to neuronal damage and is observed in inflammatory, traumatic, and neurodegenerative conditions. The events responsible for glial activation remain poorly understood; nonetheless, cytokines seem to play a major role (37, 40, 43, 67). It is conceivable that viral

replication in astrocytes results in their activation and proliferation. However, microglia did not appear to be infected; thus, we speculate that as yet unidentified signals or soluble factors elaborated by infected neurons or astrocytes trigger microglial activation. Activated microglia are increasingly recognized as important effector cells for mediating damage in a variety of experimental and natural encephalopathies (43). In HIV encephalopathy, for example, microglia are implicated in neuronal apoptosis; in other paradigms, including Theiler's virus and Sindbis infection of mice, microglia have been shown to release NO and proinflammatory cytokines (33, 41) and to express CD4 and CD8, surface molecules associated with induction of neurodegeneration (27, 42, 43).

The expression of iNOS in NBD rats was restricted to isolated macrophages at 4 weeks p.i.; thus, while NO may contribute to neuronal apoptosis, there are no data to implicate it as a major factor. Proinflammatory cytokine mRNAs, as assessed by RNase protection assay (RPA) analysis, are highest at 4 wks p.i. (25), coincident with the peak of apoptotic cell death reported in this study, suggesting a potential role of cytokines in apoptosis. Indeed, IL-1beta and TNF-alpha, both elevated in NBD rat brain, are associated with apoptosis (50, 56). In an effort to identify the source of these proinflammatory cytokines we pursued immunohistochemical analysis with antibodies to IL-1β. Only rare microglia and perivascular inflammatory cells in cerebral cortex were labeled immunohistochemically. The discordance between the RPA and IHC data for IL-1β remain unexplained; IHC studies for detection of TNFα are in progress.

IHC of activated microglia revealed expression of MHC-I, MHC-II, ICAM-1, CD4, and CD8. Whereas upregulation of MHC-II and expression of CD8 on microglial cells was transient and declined in parallel with the reduction of inflammation, high levels of ICAM-1, MHC-I, and CD4 were detected up to 76 weeks p.i. CD4 molecules were expressed on the majority of activated glial cells. In contrast, expression of CD8 was restricted to regions characterized by prominent dropout of neurons or neuronal processes. Microglial expression of CD4 is found in rats in the context of EAE and ischemia where it appears linked to expression of CNTF (19). Interestingly, RPA of NBD rat brain has not indicated upregulation of CNTF (25); thus, upregulation of CD4 is likely to reflect a different mechanism. Microglial overexpression of hCD4 in transgenic mice is associated with neuronal toxicity (8). Whether CD8 expression can be implicated in neuronal toxicity is unclear. Nonetheless, focal ischemia results in transient microglial expression of CD8 (27), and CD8 expression on cultured alveolar and peritoneal macrophages may lead to release of iNOS (24).

The NBD rat system was selected as a model for investigating mechanisms of neurodevelopmental damage in the absence of an immune response (9, 23); thus, the appearance of an extrinsic inflammatory response was not anticipated. Infiltrates comprised predominantly of CD4+ cells, CD8+ T cells, and monocytes were first detected at 2 weeks p.i., peaked at 4 weeks p.i., and decreased thereafter. However, scattered immune cells, exceeding numbers observed in control animals, were present in the brain parenchyma at the last examined timepoint, 76 weeks p.i. Transient inflammation was recently reported in neonatally infected Lewis rats (54); however, the clinical syndrome described is different than that observed here as infection was associated with severe morbidity and mortality, features more consistent with adult than neonatal BD. Although the transient appearance of inflammatory infiltrates was reproducible and coincident with the peak of neuronal apoptosis, infiltrating cells are unlikely to play a major role in neuropathogenesis. The restricted distribution of these cells to neocortex does not correlate with the pattern of neuronal damage in DG and cerebellum, where infiltrating inflammatory cells were conspicuously absent. Although infiltrating cells could potentially play a role in induction of apoptosis in cortical pyramidal neurons or through distal effects on apoptosis-related proteins in regions such as DG and cerebellum, a recent analysis of a series of neonatally thymectomized and infected Lewis rats revealed a similar pattern of apoptosis without substantive inflammation (M. Hornig and L. Stitz, unpublished). Furthermore, in contrast to adult BD, where virus-specific CD4 and CD8 T cells have been reported, it is unlikely that infiltrating T cells in the NBD model are BDV-specific. Rats in this study were inoculated within the first 12 hours of life with large intraventricular inoculi to ensure rapid drainage through cerebral sinuses to the thymus, where negative selection of the autoreactive T cell clones occurs.

Definitive proof that infiltrating T cells are not specific cannot be obtained without CTL assays; nonetheless, nonspecific recruitment of T cells into the CNS may follow expression of cytokines and adhesion and MHC molecules. Intracerebral injection of IL-1 or TNF-alpha also results in transient inflammation (11, 46). Rapid clearance of immune cells from brain following injection of IL-1, TNF-alpha, or in the context of neonatal BD presumably reflects apoptosis of these cells due

to stimulation in the absence of antigen target coupled to MHC. Finally, as noted above, studies of thymectomized animals indicate that neuronal apoptosis in neonatal BD is not dependent upon the presence of infiltrating inflammatory cells.

There is increasing interest in the notion that neuropsychiatric syndromes ranging from autism and cerebral palsy to schizophrenia represent disruptions of neurodevelopmental programs. Microbial agents, immune activation, malnutrition, and other psychological and physical stressors may be implicated in these disorders. A final common pathway that would predict targeted damage to similar structures via such disparate environmental factors might be apoptosis. The NBD rat system is a powerful model for understanding differential vulnerability of functional neural circuits and may provide new insights into the pathogenesis of CNS disorders.

Acknowledgments

This work was supported in part by NIH Grants NS29425 (W.I.L.), K08-MH01608 (M.H.), and the Austrian Fund for the Advancement of Scientific Research (H.W.). The authors thank M. Chatard, L. O'Rourke, and B. Bauder for technical assistance.

References

1. Altman J (1987) Morphological and behavioral markers of environmentally induced retardation of brain development: an animal model. *Environ Health Perspect* 74: 153-168
2. Bahmani MK, Nowrouzian I, Nakaya T, Nakamura Y, Hagiwara K, Takahashi H, Rad MA, Ikuta K (1996) Varied prevalence of Borna disease virus infection in Arabic, thoroughbred and their cross-bred horses in Iran. *Virus Res* 45: 1-13
3. Bautista JR, Rubin SA, Moran TH, Schwartz GJ, Carbone KM (1995) Developmental injury to the cerebellum following perinatal Borna disease virus infection. *Brain Res Dev Brain Res* 90: 45-53
4. Berg AL, Berg M (1998) A variant form of feline Borna disease. *J Comp Pathol* 119: 323-331
5. Berg AL, Dorries R, Berg M (1999) Borna disease virus infection in racing horses with behavioral and movement disorders. *Arch Virol* 144: 547-559
6. Briese T, Hatalski CG, Kliche S, Park YS, Lipkin WI (1995) Enzyme-linked immunosorbent assay for detecting antibodies to Borna disease virus-specific proteins. *J Clin Microbiol* 33: 348-351
7. Briese T, Schneemann A, Lewis AJ, Park YS, Kim S, Ludwig H, Lipkin WI (1994) Genomic organization of Borna disease virus. *Proc Natl Acad Sci USA* 91: 4362-4366
8. Buttini M, Westland CE, Masliah E, Yafeh AM, Wyss-Coray T, Mucke L (1998) Novel role of human CD4 molecule identified in neurodegeneration. *Nature Med* 4: 441-446
9. Carbone KM, Park SW, Rubin SA, Waltrip RW 2nd, Vogelsang GB (1991) Borna disease: association with a maturation defect in the cellular immune response. *J Virol* 65: 6154-6164
10. Chambers WH, Vujanovic NL, DeLeo AB, Olszowy MW, Herberman RB, Hiserodt JC (1989) Monoclonal antibody to a triggering structure expressed on rat natural killer cells and adherent lymphokine-activated killer cells. *J Exp Med* 169: 1373-1389
11. Claudio L, Martiney JA, Brosnan CF (1994) Ultrastructural studies of the blood-retina barrier after exposure to interleukin-1 beta or tumor necrosis factor-alpha. *Lab Invest* 70: 850-861
12. Dallman MJ, Mason DW, Webb M (1982) The roles of host and donor cells in the rejection of skin allografts by T cell-deprived rats injected with syngeneic T cells. *Eur J Immunol* 12: 511-518
13. Eisenman LM, Brothers R, Tran MH, Kean RB, Dickson GM, Dietzschold B, Hooper DC (1999) Neonatal Borna disease virus infection in the rat causes a loss of Purkinje cells in the cerebellum. *J Neurovirol* 5: 181-189
14. Flaris NA, Densmore TL, Molleston MC, Hickey WF (1993) Characterization of microglia and macrophages in the central nervous system of rats. *GLIA* 7: 34-40
15. Gavrieli Y, Sherman Y, Ben-Sasson SA (1992) Identification of programmed cell death in situ via specific labeling of nuclear DNA fragmentation. *J Cell Biol* 119: 493-501
16. Geloso MC, Vinesi P, Michetti F (1998) Neuronal subpopulations of developing rat hippocampus containing different calcium-binding proteins behave distinctively in trimethyltin-induced neurodegeneration. *Exper Neurol* 154: 645-653
17. Gonzalez-Dunia D, Eddleston M, Mackman N, Carbone K, de la Torre JC (1996) Expression of tissue factor is increased in astrocytes within the central nervous system during persistent infection with Borna disease virus. *J Virol* 70: 5812-5820
18. Gosztonyi G, Ludwig H (1995) Borna disease—neuropathology and pathogenesis. *Curr Top Microbiol Immunol* 190: 39-73
19. Hagg T, Varon S, Louis J-C (1993) Ciliary neurotrophic factor (CNTF) promotes low -affinity nerve growth factor receptor and CD4 expression by rat CNS microglia. *J Neuroimmunol* 48: 177-188
20. Hagiwara K, Kawamoto S, Takahashi H, Nakamura Y, Nakaya T, Hiramune T, Ishihara C, Ikuta K (1997) High prevalence of Borna disease virus infection in healthy sheep in Japan. *Clin Diag Lab Immunol* 4: 339-344
21. Hagiwara K, Nakaya T, Nakamura Y, Asahi S, Takahashi H, Ishihara C, Ikuta K (1996) Borna disease virus RNA in peripheral blood mononuclear cells obtained from healthy dairy cattle. *Med Microbiol Immunol (Berl)* 185: 145-151
22. Herzog S, Kompter C, Frese K, Rott R (1984) Replication of Borna disease virus in rats: age-dependent differences in tissue distribution. *Med Microbiol Immunol* 173: 171-177
23. Hirano N, Kao M, Ludwig H (1983) Persistent, tolerant or subacute infection in Borna disease virus-infected rats. *J Gen Virol* 64: 1521-1530

24. Hirji N, Lin TJ, Befus AD (1997) A novel CD8 molecule expressed by alveolar and peritoneal macrophages stimulates nitric oxide production. *J Immunol* 158: 1833-1840
25. Hornig M, Weissenböck H, Horscroft N, Lipkin WI (1999) An infection-based model of neurodevelopmental damage. *Proc Natl Acad Sci USA* 96: 12102-12107
26. Hunig T, Wallny HJ, Hartley JK, Lawetzky A, Tiefenthaler G (1989) A monoclonal antibody to a constant determinant of the rat T cell antigen receptor that induces T cell activation. Differential reactivity with subsets of immature and mature T lymphocytes. *J Exp Med* 169: 73-86
27. Jander S, Schroeter M, D'Urso D, Gillen C, Witte OW, Stoll G (1998) Focal ischemia of the rat brain elicits an unusual inflammatory response: early appearance of CD8+ macrophages/microglia. *Eur J Neurosci* 10: 680-688
28. Johnson P, Gagnon J, Barclay AN, Williams AF (1985) Purification, chain separation and sequence of the MRC OX-8 antigen, a marker of rat cytotoxic T lymphocytes. *EMBO J* 4: 2539-2545
29. Kao M, Hamir AN, Rupprecht CE, Fu ZF, Shankar V, Koprowski H, Dietzschold B (1993) Detection of antibodies against Borna disease virus in sera and cerebrospinal fluid of horses in the USA. *Vet Rec* 132: 241-244
30. Kimura H, Pickard A, Wilson DB (1984) Analysis of T cell populations that induce and mediate specific resistance to graft-versus-host disease in rats. *J Exp Med* 160: 652-658
31. Leranth C, Szeidemann Z, Hsu M, Buzsaki G (1996) AMPA receptors in the rat and primate hippocampus: a possible absence of GluR2/3 subunits in most interneurons. *Neurosci* 70: 631-652
32. Lewis AJ (1998) *Borna disease virus: molecular characterization and modulation of immunopathology*. PhD thesis, University of California Irvine, Irvine, California
33. Liang XH, Goldman JE, Jiang HH, Levine B (1999) Resistance of interleukin-1beta-deficient mice to fatal Sindbis Virus encephalitis. *J Virol* 73: 2563-2567
34. Lipkin WI, Travis GH, Carbone KM, Wilson MC (1990) Isolation and characterization of Borna disease agent cDNA clones. *Proc Natl Acad Sci USA* 87: 4184-4188
35. Ludwig H, Bode L, Gosztonyi G (1988) Borna disease: a persistent virus infection of the central nervous system. *Prog Med Virol* 35: 107-151
36. McMaster WR, Williams AF (1979) Identification of Ia glycoproteins in rat thymus and purification from rat spleen. *Eur J Immunol* 9: 426-33
37. Montero-Menei CN, Sindji L, Garcion E, Mege M, Couez D, Gamelin E, Darcy F (1996) Early events of the inflammatory reaction induced in rat brain by lipopolysaccharide intracerebral injection: relative contribution of peripheral monocytes and activated microglia. *Brain Res* 724: 55-66
38. Nakamura Y, Asahi S, Nakaya T, Bahmani MK, Saitoh S, Yasui K, Mayama H, Hagiwara K, Ishihara C, Ikuta K (1996) Demonstration of Borna disease virus RNA in peripheral blood mononuclear cells derived from domestic cats in Japan. *J Clin Microbiol* 34: 188-191
39. Narayan O, Herzog S, Frese K, Scheefers H, Rott R. (1983) Behavioral disease in rats caused by immunopathological responses to persistent Borna virus in the brain. *Science* 220: 1401-1403
40. Norenberg MD (1997) Astrocytes: normal aspects and response to CNS injury. In: *Immunology of the Nervous System*, Keane RW, Hickey WF (eds.), pp. 173-199, Oxford University Press: New York
41. Oleszak EL, Katsetos CD, Kuzmak J, Varadhachary A (1997) Inducible nitric oxide synthase in Theiler's murine encephalomyelitis virus infection. *J Virol* 71: 3228-3235
42. Perry H, Gordon S (1987) Modulation of CD4 antigen on macrophages and microglia in rat brain. *J Exp Med* 166: 1138-1143
43. Perry HV, Gordon S (1997) Microglia and macrophages. In: *Immunology of the Nervous System*., Keane RW, Hickey WF (eds.), pp. 155-172, Oxford University Press: New York
44. Pletnikov MV, Rubin SA, Vasudevan K, Moran TH, Carbone KM (1999) Developmental brain injury associated with abnormal play behavior in neonatally Borna disease virus-infected Lewis rats: a model of autism. *Behav Brain Res* 100: 43-50
45. Prehn JH, Jordan J, Ghadge GD, Preis E, Galindo MF, Roos RP, Krieglstein J, Miller RJ (1997) Ca2+ and reactive oxygen species in staurosporine-induced neuronal apoptosis. *J Neurochem* 68: 1679-1685
46. Quagliarello VJ, Wispelwey B, Long WJ Jr, Scheld WM (1991) Recombinant human interleukin-1 induces meningitis and blood-brain barrier injury in the rat. Characterization and comparison with tumor necrosis factor. *J Clin Invest* 87: 1360-1366
47. Rami A, Rabie A, Winckler J (1998) Synergy between chronic corticosterone treatment and cerebral ischemia in producing damage in noncalbindinergic neurons. *Exper Neurol* 149: 439-446
48. Richt JA, Herzog S, Haberzettl K, Rott R (1993) Demonstration of Borna disease virus-specific RNA in secretions of naturally infected horses by the polymerase chain reaction. *Med Microbiol Immunol (Berl)* 182: 293-304
49. Robinson AP, White TM, Mason DW (1986) Macrophage heterogeneity in the rat as delineated by two monoclonal antibodies MRC OX-41 and MRC OX-42, the latter recognizing complement receptor type 3. *Immunol* 57: 239-247
50. Rothwell N, Allan S, Toulmond S (1997) The role of interleukin 1 in acute neurodegeneration and stroke: pathophysiological and therapeutic implications. *J Clin Invest* 100: 2648-2652
51. Rott R, Becht H (1995) Natural and experimental Borna disease in animals. *Curr Top Microbiol Immunol* 190: 17-30
52. Rubin SA, Bautista JR, Moran TH, Schwartz GJ, Carbone KM (1999) Viral teratogenesis: brain developmental damage associated with maturation state at time of infection. *Brain Res Dev Brain Res* 112: 237-244

53. Rubin SA, Sylves P, Vogel M, Pletnikov M, Moran TH, Schwartz GJ, Carbone KM (1999) Borna disease virus-induced hippocampal dentate gyrus damage is associated with spatial learning and memory deficits. *Brain Res Bull* 48: 23-30
54. Sauder C, de la Torre JC (1999) Cytokine expression in the rat central nervous system following perinatal Borna disease virus infection. *J Neuroimmunol* 96: 29-45
55. Schneemann A, Schneider PA, Lamb RA, Lipkin WI (1995) The remarkable coding strategy of Borna disease virus: a new member of the nonsegmented negative strand RNA viruses. *Virol* 210: 1-8
56. Sei Y, Vitkovic L, Yokoyama MM (1995) Cytokines in the central nervous system: regulatory roles in neuronal function, cell death and repair. *Neuroimmunomodulation* 2: 121-133
57. Shetty AK, Turner DA (1998) Hippocampal interneurons expressing glutamic acid decarboxylase and calcium-binding proteins decrease with aging in Fischer 344 rats. *J Compar Neurol* 394: 252-269
58. Sloviter RS, Valiquette G, Abrams GM, Ronk EC, Sollas AL, Paul LA, Neubort S (1989) Selective loss of hippocampal granule cells in the mature rat brain after adrenalectomy. *Science* 243: 535-538
59. Solbrig MV, Koob GF, Joyce JN, Lipkin WI (1996) A neural substrate of hyperactivity in Borna disease: changes in brain dopamine receptors. *Virol* 222: 332-338
60. Sternberg EM, Hill JM, Chrousos GP, Kamilaris T, Listwak SJ, Gold PW, Wilder RL (1989) Inflammatory mediator-induced hypothalamic-pituitary-adrenal axis activation is defective in streptococcal cell wall arthritis-susceptible Lewis rats. *Proc Natl Acad Sci USA* 86: 2374-2378
61. Sternberg EM, Young WS, Bernardini R, Calogero AE, Chrousos GP, Gold PW, Wilder RL (1989) A central nervous system defect in biosynthesis of corticotropin-releasing hormone is associated with susceptibility to streptococcal cell wall-induced arthritis in Lewis rats. *Proc Natl Acad Sci USA* 86: 4771-4775
62. Stitz L, Dietzschold B, Carbone KM (1995) Immunopathogenesis of Borna disease. *Curr Top Microbiol Immunol* 190: 75-92
63. Toescu EC (1998) Apoptosis and cell death in neuronal cells: where does Ca2+ fit in? *Cell Calcium* 24: 387-403
64. White RA, Mason DW, Williams AF, Galfre G, Milstein C (1978) T-lymphocyte heterogeneity in the rat: separation of functional subpopulations using a monoclonal antibody. *J Exp Med* 148: 664-673
65. Williams KC, Zhao RW, Ueno K, Hickey WF (1996) PECAM-1 (CD31) expression in the central nervous system and its role in experimental allergic encephalomyelitis in the rat. *J Neurosci Res* 45: 747-757
66. Ying W (1998) Deleterious network hypothesis of apoptosis. *Med Hyp* 50: 393-398
67. Zielasek J, Hartung HP (1996) Molecular mechanisms of microglial activation. *Adv Neuroimmunol* 6: 191-222